Optical parameters of Nd^{3+}:Er^{3+}:Yb^{3+} co-doped borosilicate glasses and their energy transfers at high temperature*

Li Cheng-Ren(李成仁)[a)†], Li Shu-Feng(李淑凤)[b)], Dong Bin(董 斌)[c)], Cheng Yu-Qi(程宇琪)[a)], Yin Hai-Tao(殷海涛)[a)], Yang Jing(杨 静)[a)], and Chen Yu(陈 宇)[a)]

[a)] *College of Physics and Electronic Technology, Liaoning Normal University, Dalian* 116029, *China*
[b)] *School of Physics and Optoelectronic Technology, Dalian University of Technology, Dalian* 116024, *China*
[c)] *School of Science, Dalian Nationalities University, Dalian* 116600, *China*

(Received 8 June 2010; revised manuscript received 20 July 2010)

This paper reports that a series of Nd^{3+}:Er^{3+}:Yb^{3+} co-doped borosilicate glasses have been prepared and their absorption spectra measured. The J–O intensity parameters Ω_k (k = 2, 4, 6), spontaneous radiative lifetime $\tau_{\rm rad}$, spontaneous transition probability A, fluorescence branching ratio β and oscillator strength $f_{\rm ed}$ of the Nd^{3+} ions at room temperature are calculated based on Judd–Ofelt (J–O) theory. The temperature dependence of the up-conversion photoluminescence characteristics in a Nd^{3+}:Er^{3+}:Yb^{3+} co-doped sample is studied under a 978 nm semiconductor laser excitation, and the energy transfer mechanisms among Yb^{3+}, Er^{3+} and Nd^{3+} ions are analysed. The results show that the J–O intensity parameters Ω_2 increase when the Nd^{3+} concentration of the Nd^{3+}:Er^{3+}:Yb^{3+} co-doped borosilicate glasses increases. The possibility of spontaneous transition is small and lifetimes are long at levels of $^4F_{5/2}$ and $^4F_{3/2}$. The intensity of Nd^{3+} emissions at 595, 691, 753, 813 and 887 nm are markedly enhanced when the sample temperature exceeds 400 K. The reasons being the cooperation of the secondary sensitization from Er^{3+} to Nd^{3+} and the contribution of a multi-phonon.

Keywords: Nd^{3+}:Er^{3+}:Yb^{3+} co-doped borosilicate glasses, optical parameters, photoluminescence characteristics, high temperature

PACS: 78.55.Qr, 38.80.Wr **DOI:** 10.1088/1674-1056/20/1/017803

1. Introduction

During the last decade, the up-conversion emissions of rare-earth ion doped materials have been widely investigated due to their comprehensive application in display devices, high-density optical data reading and storage, and so on.[1−4] In particular, trivalent neodymium has abundant energy levels and much effort has been focused on it, such as for lasers and high-temperature optical sensors.[5−8] Weber investigated energy transfer between Nd^{3+} and Yb^{3+} ions in a YAl_3O_3 crystal.[9] Sousa *et al.* reported the spectroscopy properties of Nd^{3+}:Yb^{3+} co-doped fluoroindogallate glasses.[10] The up-conversion properties of Nd^{3+}-doped fluoride glass at 858 nm were investigated in detail and it was revealed that it is an efficient green emission material;[11] the up-conversion laser properties of Nd^{3+} ions were subsequently improved.[12] However, the mechanisms of energy transfer for Nd^{3+}:Er^{3+}:Yb^{3+} co-doped materials have been not reported so far. In this paper, we have prepared Nd^{3+}:Er^{3+}:Yb^{3+} co-doped borosilicate glasses by high-temperature scorching and measured their absorption spectra at 300–900 nm. The spectral characteristics of Nd^{3+}-doped borosilicate glasses in the visible and near-infrared regions have been investigated based on Judd–Ofelt (J–O) theory. The oscillator strengths of Nd^{3+} ions in Nd^{3+}:Er^{3+}:Yb^{3+} co-doped borosilicate glasses are much larger than that in Nd^{3+}: $KLa(WO_4)_2$,[13] and the spontaneous transition possibilities are smaller. The radiative lifetimes are longer in comparison to fluorophosphates glass.[14] The characteristics of up-conversion photoluminescence (PL) spectra of a Yb^{3+}:Er^{3+}:Nd^{3+} co-doped sample were discussed as a function of temperature under a 978 nm laser diode (LD) excitation. The mechanisms of energy transfer among Yb^{3+}, Er^{3+} and Nd^{3+} ions were specifically analysed. The reason for the enhancement of the PL intensities with increasing temperature is a combination of the two-stage sensiti-

*Project supported by the National Natural Science Foundation of China (Grant No. 10804015) and the Education Department of Liaoning Province, China (Grant No. 2009A417).
†Corresponding author. E-mail: lshdg@sina.com.cn
© 2011 Chinese Physical Society and IOP Publishing Ltd

sation (first Yb^{3+} to Er^{3+}, then Er^{3+} to Nd^{3+}), and the contribution of a multi-phonon. The work is helpful for the investigation of Nd^{3+} ions applied in an optical field.

2. Preparation

Er^{3+}-doped, Er^{3+}:Yb^{3+} and Nd^{3+}:Er^{3+}:Yb^{3+} co-doped borosilicate glasses have been prepared by high-temperature melting. The original compositions of the matrixes are S_iO_2, $B(OH)_3$, Na_2CO_3, $BaCO_3$. The dopant concentrations of Er^{3+}, Yb^{3+} and Nd^{3+} are 0.1 at.%, 0.5 at.% and x at.% (x = 0.1, 0.3, 0.5), which are marked with Z_1, Z_2, and Z_3, respectively. The mixed powders were sufficiently ground, homogenized and compacted in 50 mL corundum crucible and heated at 1723 K for 30 min in the high-temperature furnace. When the glass stock took on a molten state, it was cast into a preheated graphite mould to shape it and moved into another thermostat oven. Ten minutes later, the sample was taken out of the mould, put on an asbestos web and annealed at 900 K in order to eliminate the internal stress of the glass. The thermostat oven was switched off after three hours to let its temperature descend naturally to room temperature. Finally, glass samples of 25 mm×15 mm×2 mm in size were obtained after incising and polishing. Each step of the high-temperature melting, casting and annealing was carried out in an atmospheric condition.

3. Optical parameters

3.1. Absorption spectra

The absorption spectra of Nd^{3+}:Er^{3+}:Yb^{3+} co-doped borosilicate glasses were measured using a UV-visible spectrophotometer (HITACHI 200-10) in the range of 300–900 nm, as shown in Fig. 1. All of the absorption bands were similar and the absorption intensities of Er^{3+} almost remained constant because its identical Er^{3+}-doped concentration. However, the intensities of nine main absorption peaks of Nd^{3+} ions became stronger with an increase of Nd^{3+} concentration.

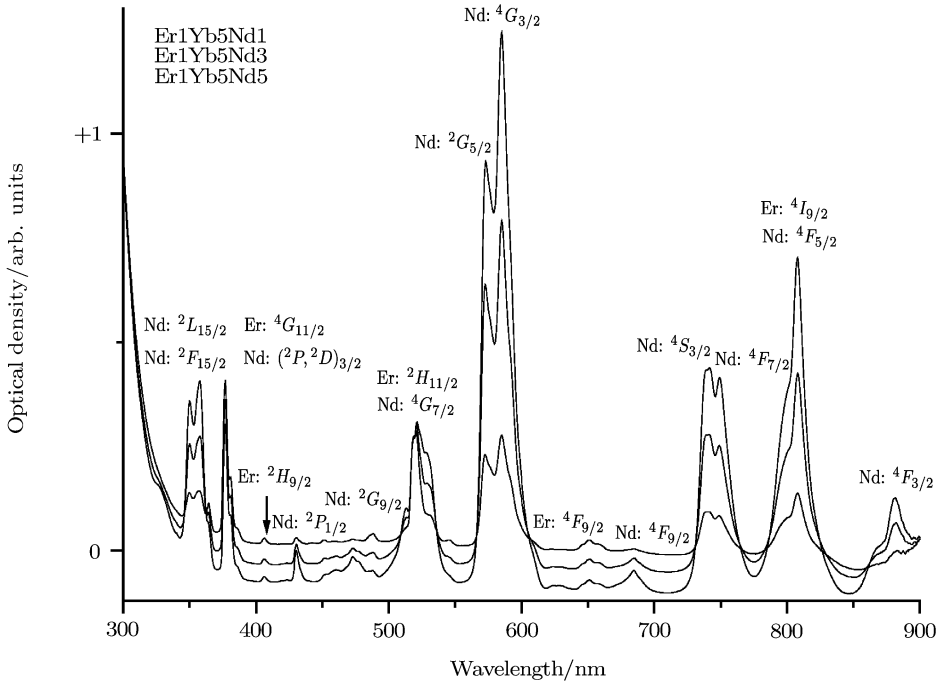


Fig. 1. The absorption spectra of the three samples.

3.2. The J–O analysis

The oscillator strength f_{ex} caused by transition, including electronic-dipole oscillator strength f_{ed} and magnetic-dipole oscillator strength f_{md}, can be calculated based on J–O theory[15,16]

$$f_{\rm ex} = f_{\rm ed} + f_{\rm md} = \frac{8\pi^2 mc}{3h\lambda(2J+1)}\frac{(n^2+2)^2}{9} \times \sum_{k=2,4,6} \Omega_k \times \langle \alpha SLJ||U^{(k)}||\alpha' S'L'J'\rangle^2 + \frac{h\sigma}{6mc}\chi \left\langle 4f^N\,\Psi J||L+2S||4f^N\,\Psi' J'\right\rangle^2, \quad (1)$$

where m, h, λ, c, J, n are electron mass, Planck constant, average wavelength of the absorption band, velocity of light, angular momentum of the ground state, and refractive index of Nd^{3+}:Er^{3+}:Yb^{3+} co-doped borosilicate glass, respectively. The refractive indexes were measured by Abbe refractometer 2WA-J in which Ar^+ laser, He–Ne laser and sodium lamp were used for light source. The refractive index of the samples at other wavelengths can be calculated by Cauchy formula. The Ω_k (k = 2, 4, 6) is J–O parameter which gives a direction to study the local structure and bonding in the neighbourhood. Of them, Ω_2 is structure/environment sensitive parameter and is known to depend on covalence and asymmetry of ion sites in vicinity, and Ω_6 is of vibronic dependence. A large value of Ω_2 is indicative of a high covalence of metal-ligand bond and Ω_6, of high rigidity. The $\left\langle \alpha SLJ||U^{(k)}||\alpha' S'L'J'\right\rangle^2$ is electronic-dipole doubly reduced matrix element of unit tensor operator $U^{(k)}$ with rank k,[17] and $\left\langle 4f^N\,\Psi J||L+2S||4f^N\,\Psi' J'\right\rangle^2$ is magnetic-dipole doubly reduced matrix element of unit tensor operator $\|L+2S\|$ for the transition within $4f$ electronic configuration.[18]

The experimental line oscillator strength is calculated using following equation:

$$f_{\rm exp}(J_1, J_2) = \frac{mc^2}{\pi e^2 NL \log {\rm e}} \int \sigma(\nu){\rm d}(\nu), \quad (2)$$

where N, L are concentrations of Nd^{3+} ions and the thickness of the samples, respectively; $\sigma(\nu)$ is optical density.

Four prominent peaks at 430, 572, 585, 739 nm, corresponding to transitions of Nd^{3+} ions from $^2P_{1/2}$, $^2G_{9/2}$, $^2G_{5/2}$ and $^4S_{3/2}$, respectively, were chosen to calculate the J–O parameters Ω_k by the least-squares fit because their absorption spectra do not overlap with Er^{3+}. It is worthwhile to point out here that the spectra were also split using Origin software for superposition parts. The results are listed in Table 1.

Table 1. Calculated J–O parameters Ω_k (k = 2, 4, 6) of samples Z_1, Z_2 and Z_3.

samples	$\Omega_2/10^{-20}$ cm^2	$\Omega_4/10^{-20}$ cm^2	$\Omega_6/10^{-20}$ cm^2	Ω_4/Ω_6
Z_1	0.0287	0.3198	0.3602	1.23
Z_2	0.0831	0.1352	0.1015	1.33
Z_3	0.1091	0.0917	0.1001	0.86

It can be found from Table 1 that the value of Ω_2 becomes larger with the increase of concentration of Nd^{3+} ions; that is, the covalence of the Nd^{3+} circumambience increases when the Nd^{3+} concentration increases, and the covalent bonding lowers the electronic levels of free ions due to nephelauxetic effect. The quality factor, defined by the ratio of Ω_4 and Ω_6, is related to odd crystalline fields and the relative intensities of the transition, and determines the nonlinear parameters of optical materials. For our glass samples, the quality factor becomes smaller with an increasing Nd^{3+} concentration, and the Ω_2 values are smaller than those reported in Refs. [19]–[21].

The root mean square deviation of the oscillator strength is obtained by

$$f_{\rm ms} = \sqrt{\sum (f_{\rm cal} - f_{\rm exp})^2/(p-q)}, \quad (3)$$

where p is the number of the spectra chosen, q is the number of the J–O parameters.

Table 2 lists measured and calculated oscillator strengths of Nd^{3+}:Er^{3+}:Yb^{3+} co-doped borosilicate glass. Both are almost the same and the root mean square deviation of the oscillator strength is quite small. However, the oscillator strength values of the samples are rather larger than that in Nd^{3+}:$KLa(WO_4)_2$.[13]

Table 2. Measured and calculated oscillator strengths of samples Z_1, $Z_2$and Z_3.

transition	wavelength/nm	Z_1	Z_2	Z_3
		oscillator strength $\times 10^{-6}$		
$^2P_{1/2} \rightarrow {}^4I_{9/2}$	430.5	$f_{\rm exp}$=0.0078	$f_{\rm exp}$=0.0049	$f_{\rm exp}$=0.0049
		$f_{\rm cal}$=0.0078	$f_{\rm cal}$=0.0049	$f_{\rm exp}$=0.0049
$^2G_{1/2} \rightarrow {}^4I_{9/2}$	572.5	$f_{\rm exp}$=0.1862	$f_{\rm exp}$=0.0913	$f_{\rm exp}$=0.0752
		$f_{\rm cal}$=0.1800	$f_{\rm cal}$=0.0890	$f_{\rm cal}$=0.0740
$^4G_{5/2} \rightarrow {}^4I_{9/2}$	583.5	$f_{\rm exp}$=0.4208	$f_{\rm exp}$=0.3347	$f_{\rm exp}$=0.3533
		$f_{\rm cal}$=0.4212	$f_{\rm cal}$=0.3349	$f_{\rm cal}$=0.3534
$^2S_{3/2} \rightarrow {}^4I_{9/2}$	739.0	$f_{\rm exp}$=0.2487	$f_{\rm exp}$=0.0971	$f_{\rm exp}$=0.0984
		$f_{\rm cal}$=0.2490	$f_{\rm cal}$=0.0917	$f_{\rm cal}$=0.0985
$f_{\rm ms}$		3.9745×10^{-9}	0.1857×10^{-9}	0.046×10^{-9}

3.3. Spontaneous transition possibility, radiative lifetime and the fluorescence branching ratio

Spontaneous transition possibility A, radiative lifetime τ and fluorescence branching ratio β can be calculated by Eqs. (4), (5) and (6) based on J–O theory,

$$A(J_1, J_2) = \frac{64\pi^4}{3h\lambda^3(2J+1)} \times \left[S_{\rm ed} n(n^2+2)^2/9 + n^3 S_{\rm md}\right], \quad (4)$$

$$\tau = \frac{1}{\sum A(J_1 \rightarrow J_2)}, \quad (5)$$

$$\beta(J_1 \rightarrow J_2) = A(J_1 \rightarrow J_2)\tau, \quad (6)$$

where $S_{\rm ed}$ and $S_{\rm md}$ are the electronic-dipole line strength and the magnetic-dipole line strength, respectively. The calculated results of Nd^{3+} ions for three samples are listed in Table 3.

Table 3. Predicted spontaneous radiation transition rates A, fluorescent branch radio β and radiation lifetimes τ of Nd^{3+} in samples Z_1, Z_2 and Z_3.

transition	λ/nm	Z_1			Z_2			Z_3		
		$A/{\rm S}^{-1}$	τ/μs	β/%	$A/{\rm S}^{-1}$	τ/μs	β/%	$A/{\rm S}^{-1}$	τ/μs	β/%
$^4F_{3/2} \rightarrow {}^4I_{15/2}$	1880	0.1766	429	0.7588	0.2443	377	0.9221	0.2676	357	0.6623
$^4F_{3/2} \rightarrow {}^4I_{13/2}$	1328	2.4271		10.429	2.6532		10.015	2.9067		13.280
$^4F_{3/2} \rightarrow {}^4I_{11/2}$	1057	8.8486		38.02	10.437		39.395	9.0031		41.128
$^4F_{3/2} \rightarrow {}^4I_{9/2}$	874.3	11.849		50.79	13.158		49.668	9.7128		44.370
$^4F_{5/2} \rightarrow {}^4F_{3/2}$	9727.6	0.3859	217	0.8375	0.4169	211	0.88	0.4216	208	1.0435
$^4F_{5/2} \rightarrow {}^4I_{15/2}$	1560.5	1.8328		3.9800	2.3991		5.051	2.4716		6.1200
$^4F_{5/2} \rightarrow {}^4I_{13/2}$	1128.6	12.871		27.930	13.201		27.79	11.591		28.690
$^4F_{5/2} \rightarrow {}^4I_{11/2}$	958.03	9.3745		20.340	9.5414		20.088	10.189		25.21
$^4F_{5/2} \rightarrow {}^4I_{9/2}$	802.2	2.1712		47.120	21.939		46.189	22.500		55.69
$^4S_{3/2} \rightarrow {}^4I_{15/2}$	1399.4	3.7619	678	25.500	4.3848	601	26.360	4.8073	581	27.91
$^4S_{3/2} \rightarrow {}^4I_{9/2}$	739.4	10.982		74.460	12.252		73.640	12.408		72.09
$^4G_{5/2} \rightarrow {}^2K_{13/2}$	583.6	0.1804	135	0.2435	0.3821	132	0.5030	0.5151	128	9.68
$^4G_{5/2} \rightarrow {}^4I_{15/2}$	902.8	0.0412		0.0556	0.0906		0.1190	0.0993		1.86
$^4G_{5/2} \rightarrow {}^4I_{13/2}$	761.4	0.7125		0.9618	1.1514		1.5150	1.2614		23.7
$^4G_{5/2} \rightarrow {}^4I_{11/2}$	661.9	23.368		3.1540	2.887		3.8000	3.1647		59.5
$^4G_{5/2} \rightarrow {}^4I_{9/2}$	550.4	70.637		95.36	71.495		94.06	75.455		14.18
$^2G_{7/2} \rightarrow {}^2K_{13/2}$	5952	11.346	325	36.93	12.055	309	37.310	13.879	289	40.2
$^2G_{7/2} \rightarrow {}^4I_{9/2}$	529.8	19.446		63.20	20.255		62.69	20.644		59.8
$^2K_{13/2} \rightarrow {}^4I_{11/2}$	593.6	0.8746	144	12.59	0.8851	136	12.04	0.9719	133	12.9
$^2K_{13/2} \rightarrow {}^2G_{7/2}$	5952.4	4.960		71.42	5.1353		69.84	5.321		70.7
$^2K_{13/2} \rightarrow {}^4G_{5/2}$	5750.4	0.0358		0.5155	0.0388		0.528	0.04		0.53
$^2K_{13/2} \rightarrow {}^4I_{9/2}$	529.8	1.0918		15.722	1.2932		17.587	1.1945		15.9

It can be seen from Table 3 that the spontaneous transition possibilities are small and that the radiative lifetimes are large at $^4F_{3/2}$ and $^4S_{3/2}$ levels. The lifetimes are longer than those of some realised Nd^{3+} doped lasers. So the samples are good candidacy materials for some optical applications.

4. Upconversion luminescence spectra at high temperature

The Nd^{3+}:Er^{3+}:Yb^{3+} co-doped borosilicate glass was placed in front of a heater, where the temperature could change from room temperature to 670 K and was monitored using a copper-constantan thermocouple with a measurement error of ±1.5 K. The pump beam of a 978 nm semiconductor laser was focused on the face of the sample. The upconversion luminescence spectra in a wavelength range of 500–950 nm were obtained from the sample, as shown in Fig. 2. The analysed spectra were collected, chopped, entered into a monochromator, detected with a CR131 photomultiplier tube equipped with a lock-in amplifier and displayed on the computer screen. The spectral resolution of the measurement system is 0.1 nm.

In Fig. 2(a), two green up-conversion emissions at about 526 and 549 nm are $^2H_{11/2} \rightarrow {}^4I_{15/2}$ and $^4S_{3/2} \rightarrow {}^4I_{15/2}$ transitions of Er^{3+} ions, respectively. The peak positions do not show a change with an increase temperature, whereas their fluorescence intensity ratio (FIR) varies and was used to measure the temperature for high-temperature environments.[22–24] It can also found from Fig. 2(a) that the spectra at 595 nm corresponding to the $^2G_{5/2} + {}^2G_{7/2} \rightarrow {}^4I_{9/2}$ transition of Nd^{3+} ions take on a clear shape and are rapidly enhanced when the temperature exceeds 545 K.

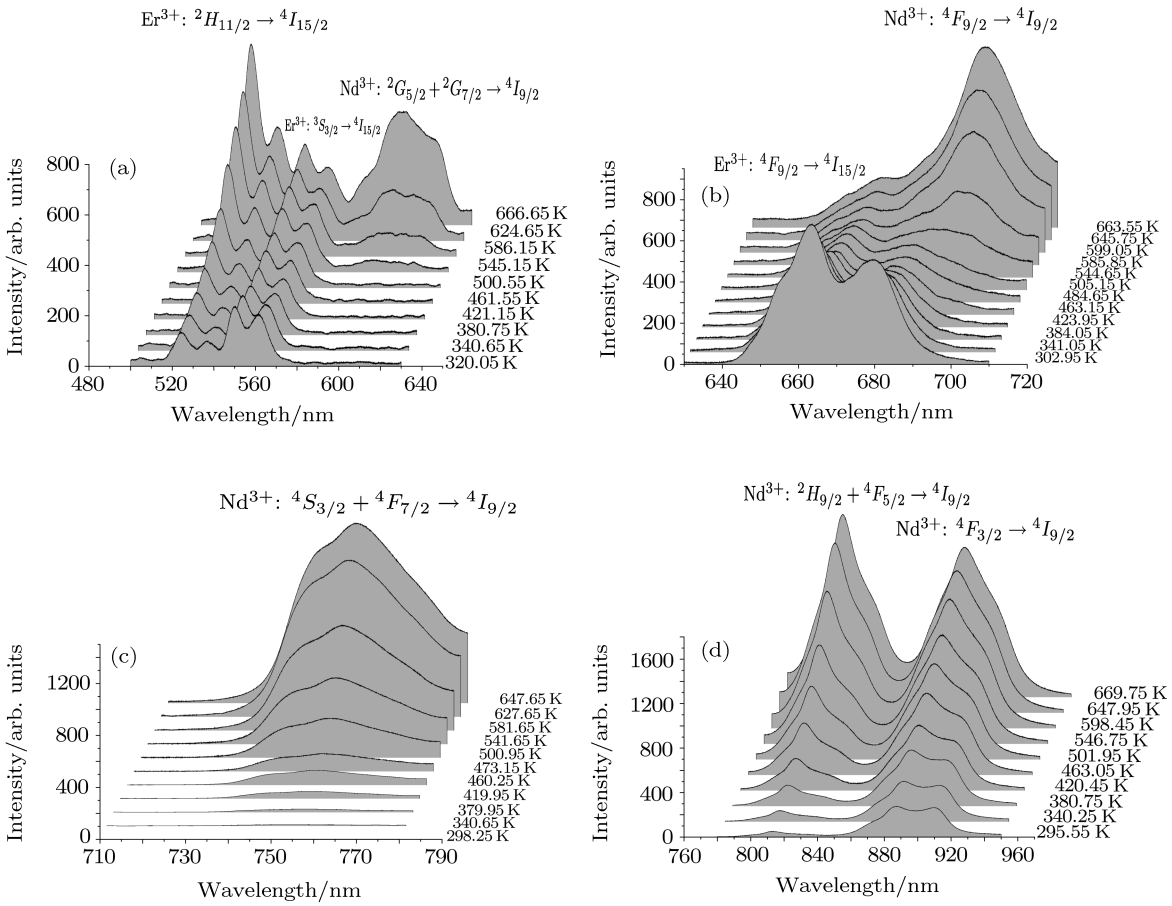


Fig. 2. The PL spectra from 500 to 960 nm of a Yb^{3+}:Er^{3+}:Nd^{3+} co-doped sample in the range of temperature about 300–667 K.

The PL intensities of the Er^{3+} ions at 664 nm, 678 nm bands attributed to the $^4F_{9/2} \rightarrow {}^4I_{15/2}$ transition get weaker with increasing temperature, as shown in Fig. 2(b). However, the spectra intensities at 691 nm that correspond to the $^4F_{9/2} \rightarrow {}^4I_{9/2}$ transitions of trivalent neodymium are getting stronger, especially after the temperature goes up to 450 K even though it is incredibly weak at room temperature. It means that energy of Er^{3+} ions at $^4F_{9/2}$ level transfers to Nd^{3+} ions at $^4F_{9/2}$ level recurring to phonons. The Er^{3+} ions are de-excited and the red up-conversion emission of Er^{3+} ions becomes progressively weaker. It also can be seen from Fig. 2(c) that the up-conversion emission at 753 nm, being $^4F_{7/2} +^4 S_{3/2} \rightarrow {}^4I_{9/2}$ transitions of Nd^{3+} ions, is monotonously enhanced with increasing temperature because the population of Nd^{3+} at levels of $^4F_{7/2}$ and $^4S_{3/2}$ dominantly originates the nonradiative decay from the $^4F_{9/2}$ level of Nd^{3+} itself, as discussed in next section. So the shapes of the PL spectra become clear when the temperature exceeds a certain value.

The transitions of Nd^{3+} ions from $^4F_{5/2} + {}^2H_{9/2}$, $^4F_{3/2}$ to $^4I_{9/2}$ radiate the PL spectra at 813 and 887 nm, respectively, as shown in Fig. 2(d). The intensities of an 813 nm emission increase more rapidly than those of 887 nm emission; while the temperature varies from 296 to 670 K and their FIR also can be used to measure high temperature.[25]

It is also known from Fig. 3 that the transitions of Er^{3+}: $^4G_{11/2} - {}^4I_{15/2}$ (380 nm), $^4F_{3/2} - {}^4I_{15/2}$ (450 nm), $^4F_{7/2} - {}^4I_{15/2}$ (488 nm), $^2H_{11/2} - {}^4I_{15/2}$ (520 nm) and $^4I_{9/2} - {}^4I_{15/2}$ (802 nm) overlap and even superpose with the transitions of Nd^{3+}: $^2P_{3/2}$, $^2D_{3/2} - {}^4I_{9/2}$, $^2P_{1/2} - {}^4I_{9/2}$, $^4G_{9/2} - {}^4I_{9/2}$, $^2G_{9/2} - {}^4I_{9/2}$ and $^4F_{5/2} - {}^4I_{9/2}$, respectively, this fact means that energy transfer between Er^{3+} and Nd^{3+} could take place within the Nd^{3+}:Er^{3+}:Yb^{3+} co-doped borosilicate glasses.

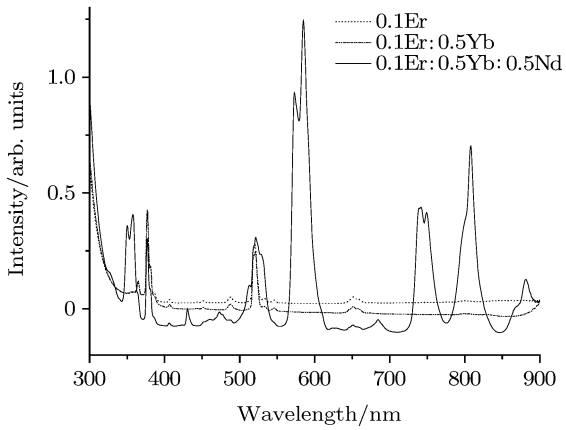


Fig. 3. The absorption spectra of Er, Er:Yb and Nd:Er:Yb borosilicate glasses.

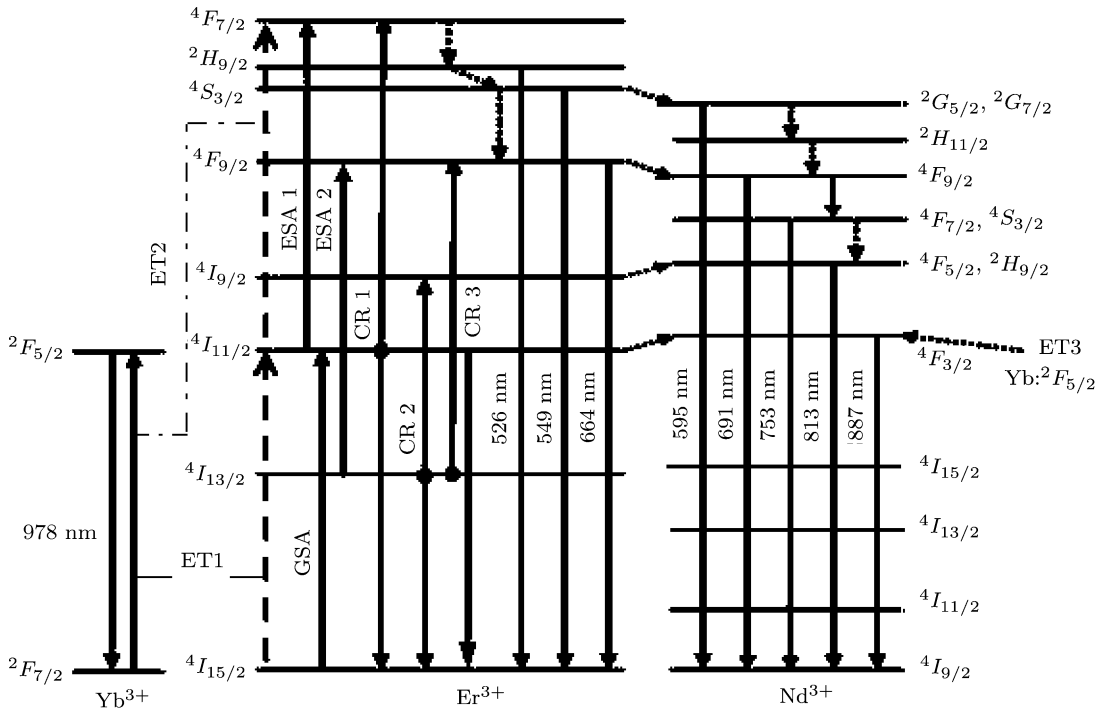


Fig. 4. Energy level diagram of Nd^{3+}:Er^{3+}:Yb^{3+} co-doped borosilicate glass excited by a 978 nm laser beam.

Figure 4 presents the schematic diagram of the energy levels of Yb^{3+}, Er^{3+}, Nd^{3+} ions and the energy transfers among them when excited by a 978 nm semiconductor laser. As can be seen, unlike Er^{3+} ion or Yb^{3+} ion, there is not an appropriate level for the Nd^{3+} ion to match absolutely the photon energy emission from 980 nm laser. Jaque *et al.*[26] discussed energy transfer mechanisms between Yb^{3+} and Nd^{3+} within a $YAl_3(BO_3)_4$ crystal with the help of multi-phonon, i.e. ET3: $^2F_{5/2}(Yb^{3+}) + {}^4I_{9/2}$ (Nd^{3+}) + phonons $\rightarrow$ $^2F_{7/2}$ (Yb^{3+}) + $^4F_{3/2}$ (Nd^{3+}). However, it is still difficult for Yb^{3+}:Nd^{3+} co-doped samples excited by a 978 nm laser to emit up-conversion PL at visible bands because there are only two levels for Yb^{3+} ions and the population density at higher excited states of Nd^{3+} ion is very small. So trivalent erbium ions are mixed into Yb^{3+}:Nd^{3+} co-doped samples in order to get more abundant spectra for Nd^{3+} ions with the help of energy transfer between Er^{3+} and Nd^{3+} ions.

Although the relatively low absorption cross-section of about 1.7×10^{-21} cm^2 makes the ground state absorption of Er^{3+} at 978 nm very weak and leads to a reduction of the emission intensity and pump efficiency, the greater absorption cross-section of about 11.7×10^{-21} cm^2 of Yb^{3+} can significantly improve the up-conversion emission properties due to its large spectral overlap and the efficient energy transfer between Yb^{3+} emission of $^2F_{5/2} \rightarrow {}^2F_{7/2}$ and Er^{3+} absorption of $^4I_{15/2} \rightarrow {}^4I_{11/2}$.[27] In other words, Yb^{3+} ions is an excellent sensitizer, not for Nd^{3+} ions, but for Er^{3+} ions. The population at each level of Er^{3+} ions could be assembled through ground state absorption (GSA), the energy transfer (ET) between Yb^{3+} and Er^{3+}, the excited state absorption (ESA) the cross-relaxation (CR) and the nonradiative decay from up-levels to down-levels.[28] The detailed processes are below:

GSA: $^4I_{15/2}$ (Er^{3+}) + a photon $\rightarrow$ $^4I_{11/2}$ (Er^{3+}),
ESA1: $^4I_{11/2}$ (Er^{3+}) + a photon $\rightarrow$ $^4F_{7/2}$ (Er^{3+}),
ESA2: $^4I_{13/2}$ (Er^{3+}) + a photon $\rightarrow$ $^4F_{9/2}$ (Er^{3+}),
CR1: $^4I_{11/2}$ (Er^{3+}) + $^4I_{11/2}$ (Er^{3+}) $\rightarrow$ $^4I_{15/2}$ (Er^{3+}) + $^4F_{7/2}$ (Er^{3+}),
CR2: $^4I_{13/2}$ (Er^{3+}) + $^4I_{13/2}$ (Er^{3+}) $\rightarrow$ $^4I_{15/2}$ (Er^{3+}) + $^4I_{9/2}$ (Er^{3+}),
CR3: $^4I_{11/2}$ (Er^{3+}) + $^4I_{13/2}$ (Er^{3+}) $\rightarrow$ $^4I_{15/2}$ (Er^{3+}) + $^4F_{9/2}$ (Er^{3+}),
ET1: $^2F_{5/2}$ (Yb^{3+}) + $^4I_{15/2}$ (Er^{3+}) $\rightarrow$ $^2F_{7/2}$ (Yb^{3+}) + $^4I_{11/2}$ (Er^{3+}),
ET2: $^2F_{5/2}$ (Yb^{3+}) + $^4I_{11/2}$ (Er^{3+}) $\rightarrow$ $^2F_{7/2}$ (Yb^{3+}) + $^4F_{7/2}$ (Er^{3+}).

Then the trivalent erbium ions act as a secondary sensitiser for Nd^{3+} ions, that is, the populations of Nd^{3+} at corresponding levels originate mainly through ET between Er^{3+} and Nd^{3+} ions recurring to multi-phonon. The process can be written as follows:

$^4S_{3/2}$ (Er^{3+}) + $^4I_{9/2}$ (Nd^{3+}) $\rightarrow$ $^4I_{15/2}$ (Er^{3+}) + $^2G_{5/2}$, $^2G_{7/2}$ (Nd^{3+}) + phonons,
$^4F_{9/2}$ (Er^{3+}) + $^4I_{9/2}$ (Nd^{3+}) $\rightarrow$ $^4I_{15/2}$ (Er^{3+}) + $^4F_{9/2}$ (Nd^{3+}) + phonons,
and $^4F_{9/2}$ (Nd^{3+}) $\rightarrow$ $^4F_{7/2}$, $^4S_{3/2}$ (Nd^{3+})+ phonons,
$^4I_{9/2}$ (Er^{3+}) + $^4I_{9/2}$ (Nd^{3+}) + phonons $\rightarrow$ $^4I_{15/2}$ (Er^{3+}) + $^4F_{5/2}$,$^2H_{9/2}$ (Nd^{3+}),
$^4I_{11/2}$ (Er^{3+}) + $^4I_{9/2}$ (Nd^{3+}) + phonons $\rightarrow$ $^4I_{15/2}$ (Er^{3+}) + $^4F_{3/2}$ (Nd^{3+}).

Subsequently, up-conversion emissions of Nd^{3+} at 595 nm ($^2G_{5/2}$+ $^2G_{7/2}$ $\rightarrow$ $^4I_{9/2}$), 691 nm ($^4F_{9/2}$ $\rightarrow$ $^4I_{9/2}$), 75 nm ($^4F_{7/2}$ + $^4S_{3/2}$ $\rightarrow$ $^4I_{9/2}$), 813 nm ($^4F_{5/2}$ + $^2H_{9/2}$ $\rightarrow$ $^4I_{9/2}$) and 887 nm ($^4F_{3/2}$ $\rightarrow$ $^4I_{9/2}$) were obtained.

Figure 5 is the logarithmic dependence of peak intensity of the up-conversion emissions as the functions of pump power. The up-conversion emission intensity ($I_{\rm up}$) is proportional to the nth power of pump power ($P_{\rm pump}$),[29] as expressed below:

$$I_{\rm up} \propto P_{\rm pump}^n,$$

where n is the number of photons required to populate the up-conversion emission states.

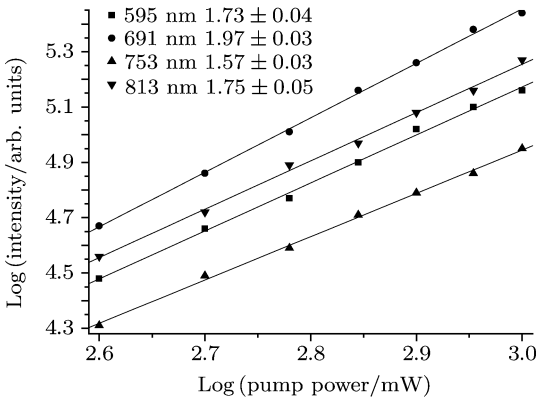


Fig. 5. Logarithmic dependence of peak intensity of the up-conversion emissions as a function of the pump power.

The experimental data of the up-conversion emission intensity are fitted to straight lines with a slope of n. The slopes are 1.73, 1.97, 1.57 and 1.75 for the emissions centred at about 595, 691, 753 and 813 nm, respectively, indicating that a two-photon process is involved for the Nd^{3+}:Er^{3+}:Yb^{3+} co-doped borosilicate glass.

5. Conclusion

Er^{3+}-doped, Er^{3+}:Yb^{3+} co-doped and Nd^{3+}:Er^{3+}:Yb^{3+} co-doped borosilicate glasses have been prepared using high-temperature scorching under solid phase, and their absorption spectra measured. The characteristics of the up-conversion PL intensity of a Nd^{3+}:Er^{3+}:Yb^{3+} co-doped sample was discussed as a function of temperature under a 978 nm semiconductor laser excitation, and the mechanisms of ET among Yb^{3+}, Er^{3+} and Nd^{3+} ions were analysed. The results show that the excitation energy of Nd^{3+} ions was obtained not only from Yb^{3+} sensitisation, but also mainly from Er^{3+} secondary sensitisation. At the same time, Nd^{3+} ions emit stronger up-conversion spectra with the increasing temperature at 595, 691, 753 and 813 nm recurring to multi-phonon. All up-conversion emissions are two-photon processes.

References

[1] Dong L Q, Huang S H, Wen H Y, Yang Y M, Wang D W and Duan X X 2009 *Acta Phys. Sin.* **58** 8617 (in Chinese)
[2] Li C R, Dong B, Li S F and Song C L 2007 *Chem. Phys. Lett.* **443** 426
[3] Chen G X, Zhang Q Y, Zhao C, Shi D M and Jiang Z H 2010 *Acta Phys. Sin.* **59** 1321 (in Chinese)
[4] Song F, Han L, Zou C, Su J, Zhang K, Yan L and Tian J 2007 *Appl. Phys.* B **86** 653
[5] Lupei V and Lupei A 2000 *Phys. Rev.* B **61** 8087
[6] Aisaka T, Fujii M and Hayashi S 2008 *Appl. Phys. Lett.* **92** 132105
[7] Huang Y H, Jiang D L, Zhang J X and Lin Q H 2010 *Acta Phys. Sin.* **59** 300 (in Chinese)
[8] Sun J C, Bian J M, Liang H O, Zhao J Z, Hu L Z, Zhao Z W, Liu W F and Du G T 2007 *Appl. Surf. Sci.* **253** 5161
[9] Weber M J 1971 *Phys. Rev.* B **4** 3153
[10] de Sousa D F, Batalioto F, Bell M J V, Oliverira and Nunes L A O 2001 *J. Appl. Phys.* **90** 3308
[11] da Gama A A S, de Sá G F, Porcher P and Caro P 1981 *J. Chem. Phys.* **75** 2583
[12] Feng Y, Song F, Zhao L J, Zhang C B, Guo H C and Zhang G Y 2001 *Acta Phys. Sin.* **50** 335 (in Chinese)
[13] Han X M and Wang G F 2002 *Mat. Res. Innovat.* **6** 235
[14] Kumar G A, de Larosa R, Matinez A, Unnikrishna N V and Ueda K 2003 *J. Phys. Chem. Solids* **64** 69
[15] Judd B R 1963 *Phys. Rev.* B **127** 750
[16] Ofelt G S 1962 *Chem. Phys.* **37** 551
[17] Weber M J 1967 *Phys. Rev.* **157** 262
[18] Leavitt R P and Morrison C A 1980 *J. Chem. Phys.* **73** 749
[19] Silva M C, Cristovan F H, Nascimento C M, Bell M J V, Cruz W O and Marletta A 2006 *J. Non-Crystalline Solids* **352** 5296
[20] Choi J H, Alfred M, Ashot M and Shi F G 2005 *J. Lumin.* **114** 167
[21] Flórez A, Martínez J F, Flórez M and Porcher P 2001 *J. Non-Crystalline Solids* **284** 261
[22] Li C R, Dong B, Li L and Lei M K 2008 *Chin. Phys.* B **17** 224
[23] Singh A K, Rai S B, Rai D K and Singh V B 2006 *Appl. Phys.* B **82** 289
[24] Dong B, Liu D P, Wang X J, Yang T, Miao S M and Li C R 2007 *Appl. Phys. Lett.* **90** 181117
[25] Li C R, Li S F Li, Dong B, Liu Z F, Song C L and Yu Q X 2008 *Sensors and Actuators* B **134** 313
[26] Jaque D, Ramirez M O, Bausá L E, Solé G J, Cavalli E, Speghini A and Bettinelli M 2003 *Phys. Rev.* B **68** 035118
[27] Vetrone F, Boyer J C and Capobianco J A 2004 *J. Appl. Phys.* **96** 661
[28] Dong B, Cao B S, Feng Q Z, Wang X J, Li C R and Hua R N 2009 *Sci. China* Ser. G **52** 1043
[29] Wade S A, Collins S F and Baxter G W 2003 *J. Appl. Phys.* **94** 4743